

Possible Enhancement of Superconductivity in Ambient-Pressure $\text{La}_3\text{Ni}_2\text{O}_7$ Thin Film

Yichen Hua,^{1,2} Wenxin He,¹ Jian-Jian Miao,^{2,*} and Changming Yue^{3,†}

¹*Department of Physics, Southern University of Science and Technology, Shenzhen 518055, China*

²*Quantum Science Center of Guangdong-Hong Kong-Macao Greater Bay Area, Shenzhen 518045, China*

³*State Key Laboratory of Quantum Functional Materials, Department of Physics,*

and Guangdong Basic Research Center of Excellence for Quantum Science,

Southern University of Science and Technology (SUSTech), Shenzhen 518055, China

As an unconventional superconducting system capable of reaching 40K under ambient pressure, the $\text{La}_3\text{Ni}_2\text{O}_7$ film superconductor has become a recent focal point in the field of superconductivity, demanding further theoretical exploration of possible pairing mechanisms. In this work, we employ the fluctuation exchange (FLEX) approximation to systematically analyze the superconducting properties of the two-orbital, two-site model for the $\text{La}_3\text{Ni}_2\text{O}_7$ film in the weakly correlated regime, focusing on its dependence on hole-doped concentration. Through a more detailed examination of the Fermi surface topology, we find that when a δ pocket composed of the d_{z^2} orbital emerges near the Γ -point, its nesting with the γ -pocket, along with the nesting between the α - and β -pockets, leads to a mutual enhancement of s_{\pm} -wave pairing at the corresponding wave vector. Furthermore, we propose that this nesting-driven enhancement of spin-fluctuation-induced pairing may be a viable mechanism to enhance superconductivity.

I. INTRODUCTION.

The mechanism of high-temperature superconductivity has long been a central research topic in condensed matter physics. In recent years, following the discovery of cuprate and iron-based superconductors, the emergence of the nickel-based superconductor family [1, 2] has attracted wide attention. Among them, Ruddlesden-Popper (RP) phase nickel-based superconductors, exemplified by the $\text{La}_3\text{Ni}_2\text{O}_7$ compound, can achieve a superconducting transition temperature of up to 80K under high pressure conditions [2]. During the past two years, significant progress has been made in both experimental characterization [3–11] and theoretical studies [12–42] of high-pressure nickel-based superconductors. One of the central questions in the theoretical study of nickel-based superconductors is how to further enhance their superconductivity, enabling them to operate at lower pressures and higher temperatures. The shape of the Fermi surface plays a critical role in determining superconducting behavior [2, 13–15]. Importantly, the Fermi surface is sensitive to variations in lattice constants, electron filling, and interaction strength [32, 42, 44, 45]. Theoretically, many research groups have explored various strategies such as chemical doping, applying pressures to tune the Fermi surface geometry and the density of states at the Fermi level, trying to enhance superconductivity [44–49].

Recently, the research team led by Z.Y.Chen achieved a breakthrough by successfully growing a $\text{La}_{2.85}\text{Pr}_{0.15}\text{Ni}_2\text{O}_7$ thin-film superconductor on an SrLaAlO_4 substrate under ambient pressure, with a superconducting transition temperature reaching about

40K [50, 51], stimulating extensive experimental and theoretical discussions regarding their superconducting mechanism [52–54]. The theoretical study by the authors [43] reveal this complex heterostructure is a moderately correlated system far from doped Mott insulator regime. Our results suggested that the superconductivity in ambient pressure $\text{La}_3\text{Ni}_2\text{O}_7$ films may originate from spin-fluctuation-induced s_{\pm} -wave pairing.

However, the significance of the ambient-pressure $\text{La}_3\text{Ni}_2\text{O}_7$ thin film superconductor extends far beyond this single material. Its study may not only guide the discovery of nickel-based superconductors with higher superconducting transition temperatures under ambient conditions, but also suggests that the structure of $\text{La}_3\text{Ni}_2\text{O}_7$ thin films can be tuned by selecting different substrates [55]. This, to some extent, alleviates the experimental difficulty of doping in nickel-based systems and provides a new platform for gaining deeper insights into the superconducting pairing mechanism [56, 57].

We find that, compared with the bulk $\text{La}_3\text{Ni}_2\text{O}_7$ compound, the $\text{La}_{2.85}\text{Pr}_{0.15}\text{Ni}_2\text{O}_7$ thin-film structure exhibits a larger inter-layer Ni–Ni distance within each bilayer, which directly reduces the inter-layer hopping t_{\perp}^z between the d_{z^2} orbitals [43]. A smaller t_{\perp}^z brings the bonding and anti-bonding states of the d_{z^2} orbital closer in energy and induces a tendency toward the emergence of a new Fermi surface. If the c -axis lattice constant can be further expanded experimentally, it would likely be favorable for enhancing the superconductivity of nickel-based systems.

In this work, we employ the fluctuation exchange (FLEX) approximation to investigate the $\text{La}_3\text{Ni}_2\text{O}_7$ thin film system in the weak coupling regime. By analyzing the Fermi surface nesting mechanism, we predicted a possible scenario that could enhance superconductivity in this system. Specifically, we first discuss the key features of the FLEX-corrected Fermi surface and spin correlation functions. We then compute and analyze the leading eigenvalue λ of the linearized Eliashberg equation

* miaojianjian@quantumsc.cn

† yuecm@sustech.edu.cn

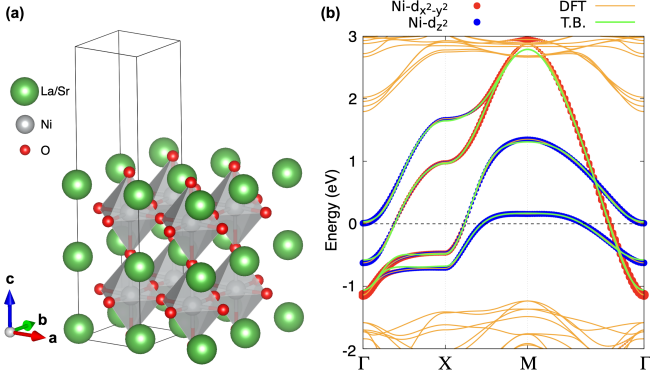


FIG. 1. (a), The schematic crystal structure of half-UC thin film of $\text{La}_3\text{Ni}_2\text{O}_7$ using the lattice parameters of $\text{La}_{2.85}\text{Pr}_{0.15}\text{Ni}_2\text{O}_7$ grown on SrLaAlO_4 substrate [51], where nickel atoms form octahedral coordination with surrounding oxygen atoms. For a better illustration, we put a exaggeratedly small vacuum than the one used in calculation above the thin film. (b), The band structure of the half-UC system. The orange lines show the DFT bands, green lines the TB bands. We also show the projected bands of the e_g orbitals, with the red (blue) dots the $d_{x^2-y^2}$ (d_{z^2}) orbital.

and its corresponding gap function on the Fermi surface, exploring possible enhance mechanisms of pairing based on the numerical behavior of λ . Finally, we summarize and discuss our findings.

II. METHOD

In this work, we simplify the complicated $\text{La}_{2.85}\text{Pr}_{0.15}\text{Ni}_2\text{O}_7/\text{SrLaAlO}_4$ heterostructure to an half-unit-cell (half-UC) $\text{La}_3\text{Ni}_2\text{O}_7$ with the experimental parameters, including the lattice constants, atomic spacing (see Ref. [43]). The minimal two-site two orbital ($d_{x^2-y^2}$ and d_{z^2} orbitals per Ni sites) model Hamiltonian is also adopted. We use A, B to label the up layer and down layer and x, z to label the orbital $d_{x^2-y^2}$ and d_{z^2} . So, the orbital basis in site representation can be expressed as $\Psi = [Ax, Az, Bx, Bz]^T$. The same Hamiltonian as in previous studies is employed [43], which can be written in momentum space, reads

$$H = H_{tb} + H_{int}, \quad (1)$$

where the tight-binding (TB) model part reads

$$H_{tb}(k) = \begin{pmatrix} T_k^x & V_k & T_k'^x & V_k' \\ V_k & T_k^z & V_k' & T_k'^z \\ T_k'^x & V_k' & T_k^x & V_k \\ V_k' & T_k'^z & V_k & T_k^z \end{pmatrix}. \quad (2)$$

Here,

$$T_k^{x/z} = 2t_1^{x/z}(\cos k_x + \cos k_y) + 2t_4^{x/z}(\cos 2k_x + \cos 2k_y) + 2t_5^{x/z}(\cos 3k_x + \cos 3k_y) + 4t_2^{x/z} \cos k_x \cos k_y + \epsilon_{x/z}, \quad (3)$$

$$T_k'^{x/z} = t_{\perp}^{x/z} + 2t_3^{x/z}(\cos k_x + \cos k_y), \quad (4)$$

$$V_k = 2t_3^{xz}(\cos k_x - \cos k_y) + 2t_5^{xz}(\cos 2k_x - \cos 2k_y), \quad (5)$$

and

$$V_k' = 2t_4^{xz}(\cos k_x - \cos k_y), \quad (6)$$

The hopping parameters can be found in Table 2 of our previous work [43]. The TB band structure is shown by the green lines in Fig. 1(b), which agrees well with the DFT one (orange line). The interaction Hamiltonian takes the Hubbard-Kanamori form, which reads

$$H_{int} = U \sum_{i, \mu} n_{i\mu\uparrow} n_{i\mu\downarrow} + U' \sum_{i, \mu < \nu, \sigma} n_{i\mu\sigma} n_{i\nu\bar{\sigma}} + (U' - J) \sum_{i, \mu < \nu, \sigma} n_{i\mu\sigma} n_{i\nu\sigma} - J \sum_{i, \mu \neq \nu} c_{i\mu\uparrow}^\dagger c_{i\mu\downarrow} c_{i\nu\downarrow}^\dagger c_{i\nu\uparrow} + J \sum_{i, \mu \neq \nu} c_{i\mu\uparrow}^\dagger c_{i\mu\downarrow}^\dagger c_{i\nu\downarrow} c_{i\nu\uparrow} \quad (7)$$

Here, U (U') is the onsite intra-orbital (inter-orbital) Coulomb interaction, and J the onsite Hund coupling and pair hopping. We assume a conventional choice for U' with $U' = U - 2J$. Furthermore, $J = U/6$ is chosen throughout this work.

FLEX is a conserving quantum many-body approximation method that self-consistently incorporates spin and charge fluctuations by summing infinite-order bubble and ladder diagrams in the self-energy calculation [58–63]. While FLEX is a perturbative approach, it has been proven highly effective in capturing the pairing symmetry driven by Fermi surface nesting. In this work, we employ the FLEX method to calculate the band renormalization of half-UC film $\text{La}_3\text{Ni}_2\text{O}_7$ system induced by interactions within the weak coupling regime. Here, only the particle-hole channel is considered. Its effective interaction is given by

$$V(q) = \frac{3}{2}U^S \chi^S(q)U^S + \frac{1}{2}U^C \chi^C(q)U^C - \frac{3}{4}U^S \chi^0(q)U^S - \frac{1}{4}U^C \chi^0(q)U^C + \frac{3}{2}U^S - \frac{1}{2}U^C \quad (8)$$

We can write the matrix element of U^S, U^C in site representation as

$$U_{ijkl}^S = \begin{cases} U, & i = j = k = l \\ U', & i = k \neq j = l \\ J, & i = j \neq k = l \\ J', & i = l \neq j = k \end{cases} \quad (9)$$

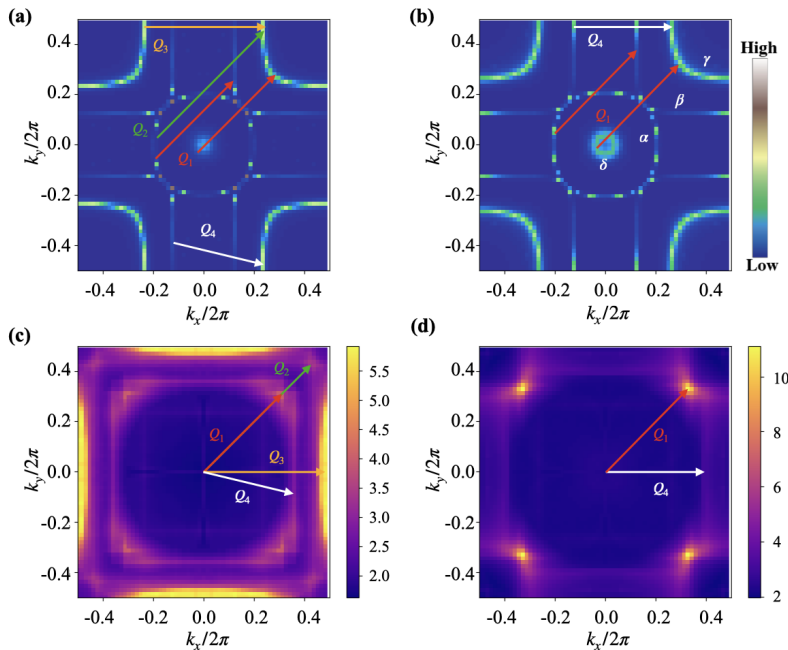


FIG. 2. The Fermi surface of $n = 1.3$ (a) and $n = 1.42$ (b). The spin susceptibility of $n = 1.3$ (c) and $n = 1.42$ (d). The four Fermi pocket named as $\delta, \alpha, \beta, \gamma$ are labeled in (b). The nesting wave vectors are marked in the corresponding figures.

$$U_{ijkl}^C = \begin{cases} U, & i = j = k = l \\ -U' + J, & i = k \neq j = l \\ 2U' - J, & i = j \neq k = l \\ J', & i = l \neq j = k \end{cases} \quad (10)$$

Please notice that only intra-layer elements are non-zero. Here, $\chi^0(q)$ is the bare susceptibility that reads $\chi_{ijkl}^0(q) = -\frac{T}{N} \sum_k G_{ki}(k) G_{jl}(k)$. $G_{ij}(k)$ is the Green's function calculated by Dyson's equation. $\chi^S(q), \chi^C(q)$ are the spin and charge susceptibilities, which can be calculated by

$$\chi^{C/S}(q) = \frac{\chi^0(q)}{1 \pm U^{C/S} \chi^0(q)}. \quad (11)$$

In this work, we use a modified code of FLEX by Witt [62]. In our calculations, we adopt a k-grid as large as 64×64 , and the temperature is fixed at $T = 0.001eV$. To ensure the validity of the FLEX approach, we restrict our discussion to cases where U is relatively small. After achieving self-consistent convergence in FLEX, the obtained physical quantities are used to solve the linearized Eliashberg equation to extract information about superconducting pairing. The self-consistent gap equation to be solved is written as

$$\lambda \Delta_{il}(k) = \frac{T}{N} \sum_q \sum_{jk} V_{ijkl}(q) F_{jk}(k-q) \quad (12)$$

where $F(k) = -G(k) \Delta(k) G^T(-\mathbf{k})$ is the anomalous Green's function, The closer the eigenvalue λ of the self-consistent equation approaches 1, the larger the instability towards the superconducting state with a certain

pairing symmetry. In previous works, we found that pairing in this system is always predominantly spin-singlet [43]. Therefore, we focus primarily on spin-singlet pairing, namely

$$V(q) = \frac{3}{2} U^S \chi^S(q) U^S - \frac{1}{2} U^C \chi^C(q) U^C + \frac{1}{4} (3U^S + U^C) \quad (13)$$

The largest eigenvalue of the linearized Eliashberg equation is efficiently computed using the power method. The pairing symmetry is analyzed from the gap function $\Delta(\mathbf{k}, i\omega_0)$ of this system, where $\omega_0 = \pi T$ is the lowest Matsubara fermi frequencies.

III. RESULTS

Since the previous computational results for the $\text{La}_3\text{Ni}_2\text{O}_7$ superconducting film indicate that the electron filling n should lie within the hole doped regime [43], we first choose two different hole doping levels for discussion. To ensure the reliability of FLEX, we set $U = 1.5$ throughout. Fig. 2 (a) and (b) illustrate the self-consistent Fermi surfaces (FS) for $n = 1.3$ and $n = 1.42$. The FS is composed of three electron pockets and one hole pocket, labeled $\delta, \alpha, \beta,$ and γ in order of increasing distance to the Γ point. As hole doping increases, the hole-like γ pocket shrinks; at $n = 1.3$, it is on the verge of vanishing. Fig. 2(c) and (d) show the largest eigenvalues of the spin susceptibility corresponding to $n = 1.3$ and $n = 1.42$, respectively. At $n = 1.3$, the spin susceptibility exhibits four distinct series of peaks, which are marked

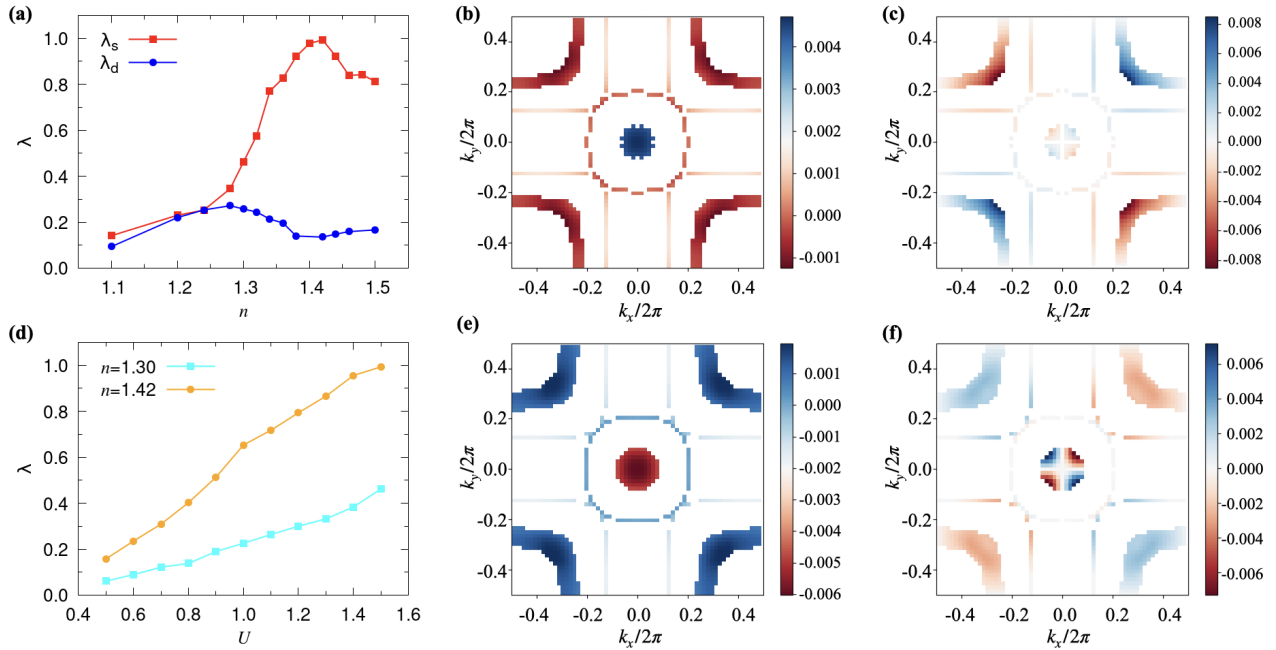


FIG. 3. (a) The λ as a function of electron filling n at $U = 1.5$, with the red line corresponding to d_{xy} -wave symmetry and the black line the s -wave symmetry. (b)-(c) The gap function of the linearized Eliashberg equation within s - and d_{xy} -wave symmetry, respectively, at $n = 1.3$. (d) The λ in s -wave symmetry as a function of U , with the red line corresponding to $n = 1.42$ and the black line $n = 1.3$. (e)-(f) The gap function of the linearized Eliashberg equation within s - and d_{xy} -wave symmetry, respectively, at $n = 1.42$.

in Fig. 2(a). Each of these peaks corresponds to a specific nesting condition in the Fermi surface: (1) Q_1 has two possible nesting contributions, one from the δ pocket to the γ pocket and the other from the α pocket to the β pocket. (2) Q_2 corresponds to the nesting from the α pocket to the γ pocket. (3) Q_3 corresponds to the nesting within the γ pocket to itself. (4) Q_4 corresponds to the nesting from the β pocket to the γ pocket. In contrast to the multi-peak structure at $n = 1.3$, the spin susceptibility at $n = 1.42$ is dominated by peaks at Q_1 and Q_4 , with the Q_1 mode being particularly pronounced. This enhancement arises from two factors. First, the γ pocket expands at $n = 1.42$, and its curvature along the diagonal direction flattens, leading to a more extended tangential region with the β pocket. Second, the nesting between the α and δ pockets improves due to better geometric congruence (i.e., the nested segments are nearly parallel). These factors cooperatively strengthen the spin fluctuations at Q_1 . Concurrently, the shrinkage and increased curvature of the γ pocket suppress the scattering channels at Q_2 and Q_3 .

Fig. 3(a) shows the variation of the eigenvalues λ for s -wave and d -wave solutions of the linearized Eliashberg equation as a function of electron filling n . It can be seen that in the over-doped hole-doped region ($n < 1.3$), both s -wave and d -wave λ values remain relatively small and exhibit competition, with the instability d -wave pairing having a slight advantage. However, in the region of lower hole doping, the s -wave eigenvalue λ_s increases sig-

nificantly with increasing n and then forming a dome-like structure near $n = 1.42$. This phenomenon can be understood by considering the FS and spin susceptibility as shown in Fig. 2, along with the gap function. Fig. 3(d) shows the variation of λ_s as a function of interaction strength U for two different doping levels. As U increases, λ_s exhibits a steady growth. Fig. 3(b) and (c) show the gap functions on the Fermi surface for s -wave and d -wave symmetries at $n = 1.3$, obtained after the power method converges and is already transformed into the band representation. Among the four types of nesting at this electron filling, only Q_3 (see Fig. 2) occurs within the intra-band, providing spin fluctuations that favor d_{xy} -wave pairing. In contrast, the other three inter-band nesting processes contribute to the possibility of s_{\pm} -wave pairing. From the gap function analysis, although the δ pocket has almost vanished, the relatively flat band near the Γ -point still generates a noticeable signal. This suggests that in the over-doped hole-doped region, there exists a competition between s_{\pm} -wave pairing, primarily driven by Q_1 and Q_4 , and d_{xy} -wave pairing, dominated by Q_3 . Fig. 3(e) and (f) show the gap functions for the s -wave and d -wave symmetries at $n = 1.42$, where this doping level is located at the dome of the $\lambda_s(n)$ which is closest to 1. Compared to the case of $n = 1.3$, the Fermi surface at this electron filling exhibits a larger density of states on the δ pocket, which matches better in size with the γ pocket. This suggests that the significant enhancement of superconductivity at this doping level is driven

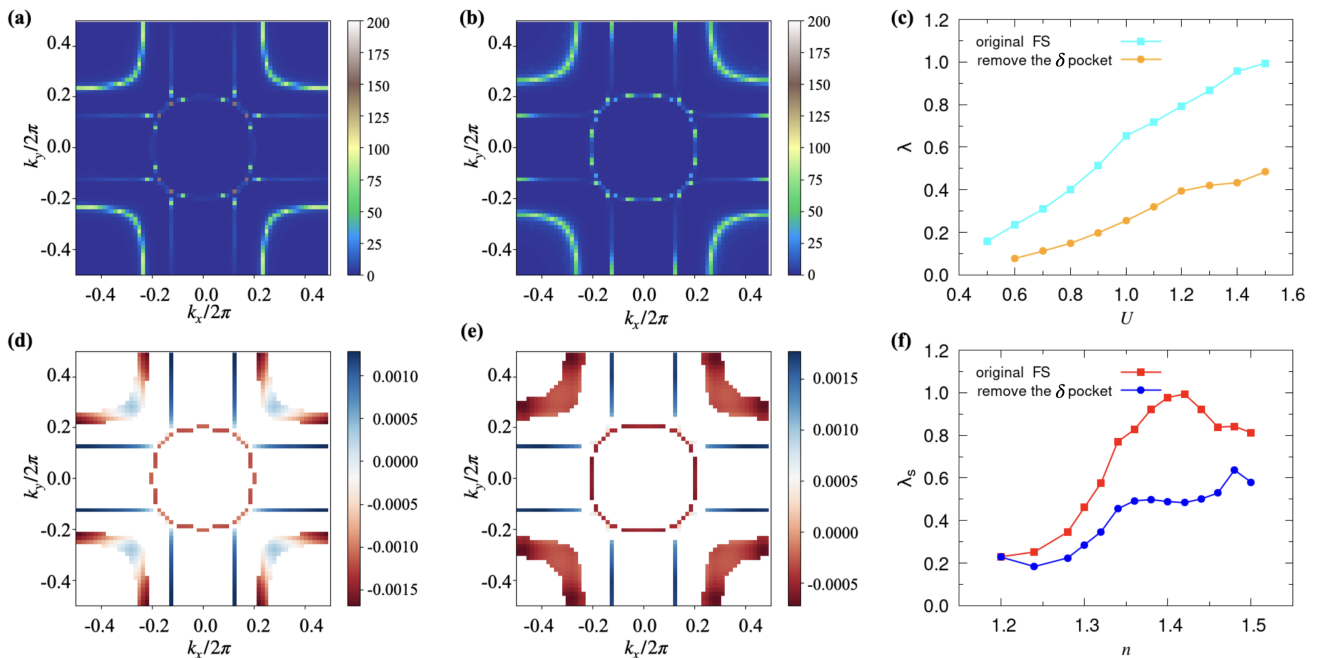


FIG. 4. (a)(b) The FS which the δ pocket is removed at $n = 1.3$ and $n = 1.42$. (d)(e) The gap function of s -wave symmetry calculated by FS like (a) and (b). (c)(f) The λ as a function of $U(n)$, $n = 1.42$ in (c) and $U = 1.5$ in (f).

by the strengthened spin fluctuations at the Q_1 wave vector, which favor pairing. However, for lower hole doping, although the shape matching between the δ pocket and the γ pocket may improve the nesting, the density of states in the δ pocket decreases due to departure from the flat band near the Γ point. Consequently, the spin fluctuations at Q_1 do not continue to increase, which may explain the presence of the dome structure at $\lambda_s(n)$.

In the previous discussion, we observed that in the weak coupling regime, the s -wave superconductivity in this system may be contributed by four types of nesting and the δ pocket appears to have a significant impact on superconductivity through the nesting with the Q_1 wave vector. To further investigate the impact of the δ pocket on superconductivity, we performed a computational experiment by artificially suppressing the Green's function spectral weight around the Γ point in the Eliashberg calculation. This allows us to isolate the specific contribution of the δ pocket to the superconducting instability. After artificially removing the δ pocket, the Fermi surfaces for $n = 1.3$ and $n = 1.42$ are shown in Fig. 4(a) and (b). We compared λ_s at $n = 1.42$ in cases where the δ pocket is present and absent, with the results shown in Fig. 4(c). The gap functions after removing the δ pocket are displayed in Fig. 4(d) and (e). The original λ_s is consistently higher than that of the case where the δ pocket is removed for all values of U , indicating that although the nesting between the α pocket and β pocket, as well as that between the γ pocket and β pocket (i.e. spin fluctuation of wave vector Q_1 and Q_3), still induce the s_{\pm} -wave pairing. However, in the presence of the δ pocket, the more stable s_{\pm} -wave pairing occurs between

the δ pocket and the γ pocket. Fig. 4(f) shows the evolution of λ_s with n in both cases, demonstrating that this enhancement remains effective across a broad hole-doped regime. Moreover, after removing the δ pocket, the dome structure previously observed at $n = 1.42$ disappears, confirming that the optimal T_c is dictated by the evolution of the d_{z^2} -derived Fermi surface near the Γ point.

IV. DISCUSSION AND CONCLUSIONS.

In this work, we used the FLEX method to study a previously proposed model Hamiltonian for the ambient pressure $\text{La}_3\text{Ni}_2\text{O}_7$ film superconductor, which is a two-site two-orbital Hubbard model. We investigated the superconducting properties of this model in the weakly correlated, hole-doped region. We conclude that the complex spin fluctuations induced by repulsive Coulomb interactions can facilitate s_{\pm} -wave pairing on the d_{z^2} orbitals, which aligns with the recent theoretical findings by Gao [64]. By examining the features of the Fermi surface and correlation functions, we discussed the impact of four spin susceptibility peaks caused by five different nesting mechanisms on superconductivity. We found that a non-trivial δ pocket in the studied band structure significantly enhances the tendency toward s_{\pm} -wave superconductivity. Furthermore, we analyzed the consistency between the Fermi surface, spin susceptibility, superconducting instability indicator λ , and the gap function as they evolve with electron filling, U . Finally, we confirmed this superconductivity enhancing mechanism by arti-

cially tuning the presence or absence of the δ pocket.

The δ band in realistic thin-film of $\text{La}_3\text{Ni}_2\text{O}_7$ ever reported tends to be away from the Fermi level. However, by slightly modifying the lattice structure through in-plane strain [65], doping or substrate substitution, the δ pocket could be "brought back" to the Fermi surface in new material realizations. If achieved in the future experiment, the presence of the δ pocket and its enhancement mechanism proposed in this study could lead to a higher

superconducting transition temperature in nickel-based superconductors.

Acknowledgements. — Changming Yue acknowledges support from the National Natural Science Foundation of China (12474231), Guangdong Provincial Quantum Science Strategic Initiative (GDZX2401004). Jian-Jian Miao is supported by NSFC (No. 12404171), the Guangdong Project (Grant No. 2024QN11X176).

-
- [1] D. Li, K. Lee, B.-Y. Wang, M. Osada, S. Crossley, H.-R. Lee, Y. Cui, Y. Hikita, H.-Y. Hwang, Superconductivity in an infinite-layer nickelate. *Nature*, 572(7771): 624-627 (2019).
- [2] H. Sun, M. Huo, X. Hu, J. Li, Z. Liu, Y. Han, L. Tang, Z. Mao, P. Yang, B. Wang, J. Cheng, D.-X. Yao, G.-M. Zhang, and M. Wang, Signatures of superconductivity near 80 K in a nickelate under high pressure, *Nature* (London) 621, 493 (2023).
- [3] J. Hou, P.-T. Yang, Z.-Y. Liu, J.-Y. Li, P.-F. Shan, L. Ma, G. Wang, N.-N. Wang, H.-Z. Guo, J.-P. Sun, *et al.*, Emergence of high-temperature superconducting phase in pressurized $\text{La}_3\text{Ni}_2\text{O}_7$ crystals, *Chin. Phys. Lett.* **40**, 117302 (2023).
- [4] Y. Zhang, D. Su, Y. Huang, Z. Shan, H. Sun, M. Huo, K. Ye, J. Zhang, Z. Yang, Y. Xu, Y. Su, R. Li, M. Smidman, M. Wang, L. Jiao, and H. Yuan, High-temperature superconductivity with zero resistance and strange-metal behaviour in $\text{La}_3\text{Ni}_2\text{O}_{7-\delta}$, *Nat. Phys.* **20**, 1269–1273 (2024).
- [5] T. Xie, M. Huo, X. Ni, F. Shen, X. Huang, H. Sun, H. C. Walker, D. Adroja, D. Yu, B. Shen, L. He, K. Cao, and M. Wang, Strong interlayer magnetic exchange coupling in $\text{La}_3\text{Ni}_2\text{O}_{7-\delta}$ revealed by inelastic neutron scattering, *Sci. Bull.* **69**, 3221–3227 (2024).
- [6] Y. Li, X. Du, Y. Cao, C. Pei, M. Zhang, W. Zhao, K. Zhai, R. Xu, Z. Liu, Z. Li, J. Zhao, G. Li, Y. Qi, H. Guo, Y. Chen, and L. Yang, Electronic correlation and pseudogap-like behavior of high-temperature superconductor $\text{La}_3\text{Ni}_2\text{O}_7$, *Chin. Phys. Lett.* **41**, 087402 (2024).
- [7] N. Wang, G. Wang, X. Shen, J. Hou, J. Luo, X. Ma, H. Yang, L. Shi, J. Dou, J. Feng, J. Yang, Y. Shi, Z. Ren, H. Ma, P. Yang, Z. Liu, Y. Liu, H. Zhang, X. Dong, Y. Wang, K. Jiang, J. Hu, S. Nagasaki, K. Kitagawa, S. Calder, J. Yan, J. Sun, B. Wang, R. Zhou, Y. Uwatoko, J. Cheng, Bulk high-temperature superconductivity in pressurized tetragonal $\text{La}_2\text{PrNi}_2\text{O}_7$, *Nature* **634**, 579-584 (2024).
- [8] D. Zhao, Y. Zhou, M. Huo, Y. Wang, L. Nie, Y. Yang, J. Ying, M. Wang, T. Wu, and X. Chen, Pressure-enhanced spin-density-wave transition in double-layer nickelate $\text{La}_3\text{Ni}_2\text{O}_{7-\delta}$, *Science Bulletin* (2025).
- [9] G. Wang, N. N. Wang, X. L. Shen, J. Hou, L. Ma, L. F. Shi, Z. A. Ren, Y. D. Gu, H. M. Ma, P. T. Yang, *et al.*, Pressure-Induced Superconductivity in Polycrystalline $\text{La}_3\text{Ni}_2\text{O}_{7-\delta}$, *Phys. Rev. X* **14**, 011040 (2024).
- [10] S. Cai, Y. Zhou, H. Sun, K. Zhang, J. Zhao, M. Huo, L. Nataf, Y. Wang, J. Li, J. Guo, *et al.*, Low-temperature mean valence of nickel ions in pressurized $\text{La}_3\text{Ni}_2\text{O}_7$, *Phys. Rev. B* **111**, 104511 (2025).
- [11] Z. Liu, M. Huo, J. Li, Q. Li, Y. Liu, Y. Dai, X. Zhou, J. Hao, Y. Lu, M. Wang, *et al.*, Electronic correlations and partial gap in the bilayer nickelate $\text{La}_3\text{Ni}_2\text{O}_7$, *Nat. Commun.* **15**, 7570 (2024).
- [12] Zhihui Luo, Xunwu Hu, Meng Wang, Wei Wu, and Dao-Xin Yao, Bilayer Two-Orbital Model of $\text{La}_3\text{Ni}_2\text{O}_7$ under Pressure, *Physical Review Letters* **131**, 126001 (2023).
- [13] Q.-G. Yang, D. Wang, and Q.-H. Wang, Possible s^\pm -wave superconductivity in $\text{La}_3\text{Ni}_2\text{O}_7$, *Phys. Rev. B* **108**, L140505 (2023).
- [14] Y.-B. Liu, J.-W. Mei, F. Ye, W.-Q. Chen, and F. Yang, s^\pm -Wave Pairing and the Destructive Role of Apical-Oxygen Deficiencies in $\text{La}_3\text{Ni}_2\text{O}_7$ under Pressure, *Phys. Rev. Lett.* **131**, 236002 (2023).
- [15] Y.-F. Yang, G.-M. Zhang, and F.-C. Zhang, Interlayer valence bonds and two-component theory for high- T_c superconductivity of $\text{La}_3\text{Ni}_2\text{O}_7$ under pressure, *Phys. Rev. B* **108**, L201108 (2023).
- [16] Q. Qin and Y.-F. Yang, High- T_c superconductivity by mobilizing local spin singlets and possible route to higher T_c in pressurized $\text{La}_3\text{Ni}_2\text{O}_7$, *Phys. Rev. B* **108**, L140504 (2023).
- [17] Y. Zhang, L.-F. Lin, A. Moreo, and E. Dagotto, Electronic structure, dimer physics, orbital-selective behavior, and magnetic tendencies in the bilayer nickelate superconductor $\text{La}_3\text{Ni}_2\text{O}_7$ under pressure, *Phys. Rev. B* **108**, L180510 (2023).
- [18] Viktor Christiansson, Francesco Petocchi, and Philipp Werner, Correlated Electronic Structure of $\text{La}_3\text{Ni}_2\text{O}_7$ under Pressure, *Phys. Rev. Lett.* **131**, 206501 (2023).
- [19] P. Puphal, P. Reiss, N. Enderlein, Y.-M. Wu, G. Khalullin, V. Sundaramurthy, T. Priessnitz, M. Knauff, A. Suthar, L. Richter, *et al.*, Unconventional crystal structure of the high-pressure superconductor $\text{La}_3\text{Ni}_2\text{O}_7$, *Phys. Rev. Lett.* **133**, 146002 (2024).
- [20] Z. Liao, L. Chen, G. Duan, Y. Wang, C. Liu, R. Yu, and Q. Si, Electron correlations and superconductivity in $\text{La}_3\text{Ni}_2\text{O}_7$ under pressure tuning, *Phys. Rev. B* **108**, 214522 (2023).
- [21] Z. Liao, Y. Wang, L. Chen, G. Duan, R. Yu, and Q. Si, Orbital-selective electron correlations in high- T_c bilayer nickelates: from a global phase diagram to implications for spectroscopy, arXiv:2412.21019 (2024).
- [22] Y. Zhang, L.-F. Lin, A. Moreo, T. A. Maier, and E. Dagotto, Electronic structure, self-doping, and superconducting instability in the alternating single-layer trilayer stacking nickelates $\text{La}_3\text{Ni}_2\text{O}_7$, *Phys. Rev. B* **110**, L060510 (2024).
- [23] Y. Zhang, L.-F. Lin, A. Moreo, T. A. Maier, and E. Dagotto, Trends in electronic structures and s^\pm -wave pairing for the rare-earth series in bilayer nickelate super-

- conductor $R_3Ni_2O_7$, *Phys. Rev. B* **108**, 165141 (2023).
- [24] Y.-H. Tian, Y. Chen, J.-M. Wang, R.-Q. He, and Z.-Y. Lu, Correlation effects and concomitant two-orbital s^\pm -wave superconductivity in $La_3Ni_2O_7$ under high pressure, *Phys. Rev. B* **109**, 165154 (2024).
- [25] H. Yang, H. Oh, and Y.-H. Zhang, Strong pairing from a small Fermi surface beyond weak coupling: Application to $La_3Ni_2O_7$, *Phys. Rev. B* **110**, 104517 (2024).
- [26] Z. Fan, J.-F. Zhang, B. Zhan, D. Lv, X.-Y. Jiang, B. Normand, and T. Xiang, *Superconductivity in nickelate and cuprate superconductors with strong bilayer coupling*, *Phys. Rev. B* **110**, 024514 (2024).
- [27] Siheon Ryee, Niklas Witt, and Tim O. Wehling, Quenched Pair Breaking by Interlayer Correlations as a Key to Superconductivity in $La_3Ni_2O_7$, *Phys. Rev. Lett.* **133**, 096002 (2024).
- [28] Y. Wang, K. Jiang, Z. Wang, F.-C. Zhang, and J. Hu, Electronic and magnetic structures of bilayer $La_3Ni_2O_7$ at ambient pressure, *Phys. Rev. B* **110**, 205122 (2024).
- [29] X. Chen, J. Choi, Z. Jiang, J. Mei, K. Jiang, J. Li, S. Agrestini, M. Garcia-Fernandez, H. Sun, X. Huang, *et al.*, Electronic and magnetic excitations in $La_3Ni_2O_7$, *Nat. Commun.* **15**, 9597 (2024).
- [30] C. Lu, Z. Pan, F. Yang, and C. Wu, Interlayer-coupling-driven high-temperature superconductivity in $La_3Ni_2O_7$ under pressure, *Phys. Rev. Lett.* **132**, 146002 (2024).
- [31] H. Sakakibara, N. Kitamine, M. Ochi, and K. Kuroki, Possible high T_c superconductivity in $La_3Ni_2O_7$ under high pressure through manifestation of a nearly half-filled bilayer Hubbard model, *Phys. Rev. Lett.* **132**, 106002 (2024).
- [32] K. Jiang, Z. Wang, and F.-C. Zhang, High-temperature superconductivity in $La_3Ni_2O_7$, *Chin. Phys. Lett.* **41**, 017402 (2024).
- [33] J.-X. Zhang, H.-K. Zhang, Y.-Z. You, and Z.-Y. Weng, Strong pairing originated from an emergent Z_2 Berry phase in $La_3Ni_2O_7$, *Phys. Rev. Lett.* **133**, 126501 (2024).
- [34] Y.-Y. Zheng and W. Wu, s^\pm -wave superconductivity in the bilayer two-orbital Hubbard model, *Phys. Rev. B* **111**, 035108 (2025).
- [35] P. Puphal, T. Schäfer, B. Keimer, and M. Hepting, Superconductivity in infinite-layer and Ruddlesden–Popper nickelates, *Nat. Rev. Phys.* 1–16 (2025).
- [36] K.-Y. Jiang, Y.-H. Cao, Q.-G. Yang, H.-Y. Lu, and Q.-H. Wang, Theory of pressure dependence of superconductivity in bilayer nickelate $La_3Ni_2O_7$, *Physical Review Letters.* **134** 076001 (2025).
- [37] G. Duan, Z. Liao, L. Chen, Y. Wang, R. Yu, and Q. Si, Orbital-selective correlation effects and superconducting pairing symmetry in a multiorbital t - J model for bilayer nickelates, arXiv:2502.09195 (2025).
- [38] W. Xi, S.-L. Yu, and J.-X. Li, Transition from s^\pm -wave to $d_{x^2-y^2}$ -wave superconductivity driven by interlayer interaction in the bilayer two-orbital model of $La_3Ni_2O_7$, *Phys. Rev. B* **111**, 104505 (2025).
- [39] L. Shi, Y. Luo, W. Wu, and Y. Zhang, Theoretical Investigation of High- T_c Superconductivity in Sr-Doped $La_3Ni_2O_7$ at Ambient Pressure, arXiv preprint arXiv:2503.13197 (2025).
- [40] Z. Ouyang, R.-Q. He, and Z.-Y. Lu, Two key factors to superconductivity of Ruddlesden-Popper nickelates: enhanced quasi-particle weight and strong local spin fluctuation, arXiv preprint arXiv:2503.08682 (2025).
- [41] T. A. Maier, P. Doak, L.-F. Lin, Y. Zhang, A. Moreo, and E. Dagotto, Interlayer pairing in bilayer nickelates, *npj Quantum Materials* (2026).
- [42] Wang Y, Zhang Y, Jiang K. Electronic structure and disorder effect of $La_3Ni_2O_7$ superconductor[J]. *Chinese Physics B*, 2025, 34(4): 047105.
- [43] C. Yue, J.-J. Miao, H. Huang, Y. Hua, P. Li, Y. Li, G. Zhou, W. Lv, Q. Yang, F. Yang, *et al.*, Correlated electronic structures and unconventional superconductivity in bilayer nickelate heterostructures, *Natl. Sci. Rev.*, nwaf253 (2025).
- [44] S. Wu, Z. Yang, X. Ma, J. Dai, M. Shi, H.-Q. Yuan, H.-Q. Lin, and C. Cao, $Ac_3Ni_2O_7$ and $La_2AeNi_2O_6F$ ($Ae = Sr, Ba$): Benchmark materials for bilayer nickelate superconductivity, arXiv:2403.11713 (2024).
- [45] Huo Z, Luo Z, Zhang P, Yang A, Liu Z, Tao X, Zhang Z, Guo S, Jiang Q, Chen W, et al. Modulation of the octahedral structure and potential superconductivity of $La_3Ni_2O_7$ through strain engineering[J]. *Science China Physics, Mechanics Astronomy*, 2025, 68(3): 237411 (2025).
- [46] Wang G, Wang N, Wang Y, Shi L, Shen X, Hou J, Ma H, Yang P, Liu Z, Zhang H, et al. Observation of high-temperature superconductivity in the high-pressure tetragonal phase of $La_2PrNi_2O_{7-\delta}$ [J]. arXiv preprint arXiv:2311.08212, 2023.
- [47] Rhodes L C, Wahl P. Structural routes to stabilize superconducting $La_3Ni_2O_7$ at ambient pressure[J]. *Physical Review Materials*, 2024, 8(4): 044801.
- [48] Geisler B, Hamlin J J, Stewart G R, Hennig R G, Hirschfeld P J. Structural transitions, octahedral rotations, and electronic properties of $A_3Ni_2O_7$ rare-earth nickelates under high pressure[J]. *npj Quantum Materials*, 2024, 9(1): 38.
- [49] Chen X, Jiang P, Li J, Zhong Z, Lu Y. Charge and spin instabilities in superconducting $La_3Ni_2O_7$ [J]. *Physical Review B*, 2025, 111(1): 014515 (2025).
- [50] E. Ko, Y. Yu, Y. Liu, L. Bhatt, J. Li, V. Thampy, C. Kuo, B. Wang, Y. Lee, K. Lee, J. Lee, B. H. Goodge, D. A. Muller, H. Y. Hwang, Signatures of ambient pressure superconductivity in thin film $La_3Ni_2O_7$, *Nature* (2024).
- [51] G. Zhou, W. Lv, H. Wang, Z. Nie, Y. Chen, Y. Li, H. Huang, W.-Q. Chen, Y.-J. Sun, Q.-K. Xue, *et al.*, Ambient-pressure superconductivity onset above 40 K in $(La, Pr)_3Ni_2O_7$ films, *Nature* **640**, 641–646 (2025).
- [52] Y. Liu, E. K. Ko, Y. Tarn, L. Bhatt, J. Li, V. Thampy, B. H. Goodge, D. A. Muller, S. Raghu, Y. Yu, *et al.*, Superconductivity and normal-state transport in compressively strained $La_2PrNi_2O_7$ thin films, *Nature Materials*, 1–7 (2025).
- [53] J. Yang, H. Sun, X. Hu, Y. Xie, T. Miao, H. Luo, H. Chen, B. Liang, W. Zhu, G. Qu, C.-Q. Chen, M. Huo, Y. Huang, S. Zhang, F. Zhang, F. Yang, Z. Wang, Q. Peng, H. Mao, G. Liu, Z. Xu, T. Qian, D.-X. Yao, M. Wang, L. Zhao, X. J. Zhou, Orbital-dependent electron correlation in double-layer nickelate $La_3Ni_2O_7$, *Nat. Commun.* **15**, 4373 (2024).
- [54] P. Li, G. Zhou, W. Lv, Y. Li, C. Yue, H. Huang, L. Xu, J. Shen, Y. Miao, W. Song, *et al.*, Angle-resolved photoemission spectroscopy of superconducting $(La, Pr)_3Ni_2O_7/SrLaAlO_4$ heterostructures, *Natl. Sci. Rev.*, nwaf205 (2025).
- [55] M. Osada, C. Terakura, A. Kikkawa, M. Nakajima, H.-Y. Chen, Y. Nomura, Y. Tokura, and A. Tsukazaki, Strain-tuning for superconductivity in $La_3Ni_2O_7$ thin

- films, *Commun. Phys.* **8**, 251 (2025).
- [56] B. Hao, M. Wang, W. Sun, Y. Yang, Z. Mao, S. Yan, H. Sun, H. Zhang, L. Han, Z. Gu, *et al.*, Superconductivity in Sr-doped $\text{La}_3\text{Ni}_2\text{O}_7$ thin films, *Nature Materials* **24**, 1756–1762 (2025).
- [57] Y. Wang, K. Jiang, J. Ying, T. Wu, J. Cheng, J. Hu, and X. Chen, Recent progress in nickelate superconductors, *Natl. Sci. Rev.* **12**, nwaf373 (2025).
- [58] N. E. Bickers and D. J. Scalapino, Conserving approximations for strongly fluctuating electron systems. I. Formalism and calculational approach, *Ann. Phys.* **193**, 206–251 (1989).
- [59] N. E. Bickers and S. R. White, Conserving approximations for strongly fluctuating electron systems. II. Numerical results and parquet extension, *Phys. Rev. B* **43**, 8044 (1991).
- [60] Y. Yanase, T. Jujo, T. Nomura, H. Ikeda, T. Hotta, and K. Yamada, Theory of superconductivity in strongly correlated electron systems, *Phys. Rep.* **387**, 1–149 (2003).
- [61] K. Kuroki, S. Onari, R. Arita, H. Usui, Y. Tanaka, H. Kontani, and H. Aoki, Unconventional Pairing Originating from the Disconnected Fermi Surfaces of Superconducting $\text{LaFeAsO}_{1-x}\text{F}_x$, *Phys. Rev. Lett.* **101**, 087004 (2008).
- [62] N. Witt, E. G. C. P. Van Loon, T. Nomoto, R. Arita, and T. O. Wehling, Efficient fluctuation-exchange approach to low-temperature spin fluctuations and superconductivity: From the Hubbard model to $\text{Na}_x\text{CoO}_2 \cdot y\text{H}_2\text{O}$, *Phys. Rev. B* **103**, 205148 (2021).
- [63] K. Björnson, A. Kreisel, A. T. Rømer, and B. M. Andersen, Orbital-dependent self-energy effects and consequences for the superconducting gap structure in multi-orbital correlated electron systems, *Phys. Rev. B* **103**, 024508 (2021).
- [64] Y. Gao, Theoretical study of the electronic correlation and superconducting pairing in $\text{La}_{2.85}\text{Pr}_{0.15}\text{Ni}_2\text{O}_7$ film grown on SrLaAlO_4 , arXiv:2507.19784 (2025).
- [65] Y.-H. Cao, K.-Y. Jiang, H.-Y. Lu, D. Wang, Q.-H. Wang, arXiv:2507.13694 (2025).